About 3D Cavity Resonance

May 14, 2026
July 7, 2026 Revised
Takuya Yabu(takuya.yabu@live.jp)

Abstract

Research on automobile whistling and suction sounds has been conducted in the past. For cavity resonance, a type of whistling sound, the cavity resonance frequency has been determined using Rossiter's empirical equation. Therefore, we limited our study to the three-dimensional case and clarified the physical phenomena that arise by solving a set of partial differential equations that explain the phenomenon. As a result, we were able to determine the frequency at which resonance increases, taking into account three-dimensional space. Finally, we were able to confirm the conditions under which resonance increases through numerical calculations.

Nomenclature

L_x, L_y, L_z: Size of the hole in the x, y, and z directions.
ρ, c: Air density and air sound speed
ω: Angular frequency
f_x, f_y, f_z: Resonance frequencies in the x, y, and z directions
k: Wavenumber
t: Time
j: Imaginary unit
U, U_{vx}: Mainstream air velocity and vortex (vorticity) velocity
κ: Ratio of vortex (vorticity) velocity to mainstream air velocity
ϕ: Empirical coefficient for phase lag
M: Mach number
ζ: Vorticity
β: Efficiency of conversion from sound pressure to vorticity
$\delta(x)$: Dirac delta function
$\delta'(x)$: Differential of Dirac delta function
$H(x)$: Heaviside step function
$u(x,y,z,t), v(x,y,z,t), w(x,y,z,t)$: Velocity in the x, y, and z directions

1. Introduction

In the past, research has been conducted on the whistling and suction sounds of automobiles (Calvo, Diaz, & San Roman, 2005) (Chien-Hsiung, Lung-Ming , Chang-Hsien , Yen-Loung , & Jik-Chang , 2009) (George, 1990) (Jagtiani, 1972) (Jung & Oh, 1995) (Münder & Carbon, 2022) (Oettle & Sims-Williams, 2017) (Qatu, Abdelhamid, Pang, & Sheng, 2009) (Wang, Chen, & Zhang, 2021) (Zhang, Meng, Li, & Zheng, 2022). Cavity resonance is a type of whistling sound. In cavity resonance, the cavity resonance frequency has traditionally been determined using Rossiter formula, an empirical formula. Therefore, for cavity resonance in the three-dimensional case, we will clarify the physical phenomena that arise by solving the set of partial differential equations that explain the phenomenon. Finally, we will examine the conditions under which resonance increases in numerical calculations.

These will be discussed below.

2. About 3D Cavity Resonance

2.1. Vorticity Movement Equation

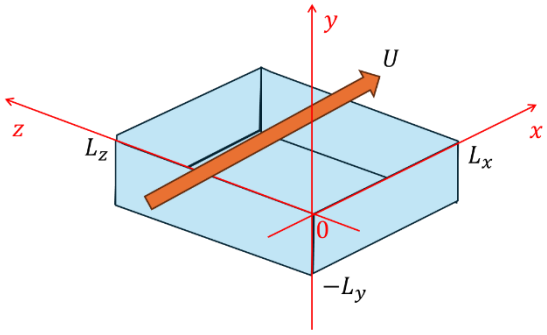

Fig. 1 3-Dimensional Box with Hole

Fig. 1 shows a box with a hole. Here, the conventional definitions of cavity resonance and cavity resonance frequency are given below.

Definition：

When air is flowing at velocity U and there is a hole, a vortex moves from the upstream end to the downstream end of the hole. This vortex collides with the downstream end, generating sound. This generated sound then moves from the downstream end to the upstream end. Sound is a change accompanied by particle velocity, and this particle velocity then collides with the upstream end, generating another vortex. This series of phenomena is

defined as "cavity resonance." Furthermore, the reciprocal of the time from when a vortex moves and generates sound until another vortex is generated is defined as the "cavity resonance frequency."

Based on this definition, we derive the differential equation representing cavity resonance, limited to three dimension. First, the movement equation of vorticity $\zeta_z(x,y,z,t)$ is expressed by the following equation. However, the viscosity term is ignored. Furthermore, $\zeta_z(x,y,z,t)$ is the vorticity around the z-axis.

$$\frac{\partial \zeta_z}{\partial t} + U_{vx}\frac{\partial \zeta_z}{\partial x} = 0 \tag{1}$$

2.2. Powell's Equation

Next, we will find the relationship between sound pressure and vorticity.

Powell's equation is the relationship between sound pressure and vorticity. Expressed in three dimension, Powell's equation is given by the following:

$$\begin{aligned}&\frac{1}{c^2}\frac{\partial^2 p}{\partial t^2} - \left(\frac{\partial^2 p}{\partial x^2} + \frac{\partial^2 p}{\partial y^2} + \frac{\partial^2 p}{\partial z^2}\right)\\ &= \rho[\zeta_z(L_x,0,0,t)u(L_x,0,0,t)\delta'(x-L_x)\delta(y)\delta(z)\\ &\quad -\zeta_z(L_x,0,0,t)v(L_x,0,0,t)\delta(x-L_x)\delta'(y)\delta(z)]\end{aligned} \tag{2}$$

2.3. Initial Conditions

The initial condition for the velocity in the x-direction is given below:

$$u(x, y \geq 0, 0) = U \tag{3}$$

The initial condition for the velocity in the y-direction is given below:

$$v(x,y,0) = 0 \tag{4}z$$

The initial condition for the velocity in the z-direction is given below:

$$w(x,y,z,0) = 0 \tag{5}$$

The initial condition for the sound pressure is given below:

$$p(x,y,0) = 0 \tag{6}$$

The initial condition for the time derivative of the sound pressure is given below:

$$\left.\frac{\partial p}{\partial t}\right|_{t=0} = 0 \tag{7}$$

2.4. Boundary Conditions

We need to find the boundary conditions under which the velocity of the returned

particles changes to vorticity. These are given by the following equation:

$$\zeta(0,0,0 \le z \le L_z,t) = -\beta_x \left.\frac{\partial p}{\partial x}\right|_{(x=0,y=0,t=t)} \tag{8}$$

Furthermore, assuming that sound pressure is completely reflected at the bottom of the box and becomes zero at the open end, the following conditions hold true.

$$\left.\frac{\partial p}{\partial x}\right|_{y=-L_y} = 0 \tag{9}$$

$$p|_{y=0} = 0 \tag{10}$$

Furthermore, assuming that the sound pressure is completely reflected by the front and back walls, the following conditions hold true.

$$\left.\frac{\partial p}{\partial x}\right|_{x=0,-L_y \le y \le 0} = 0 \tag{11}$$

$$\left.\frac{\partial p}{\partial x}\right|_{x=L_H,-L_y \le y \le 0} = 0 \tag{12}$$

Furthermore, assuming that the sound pressure is completely reflected by the left and right walls, the following conditions hold true.

$$\left.\frac{\partial p}{\partial z}\right|_{z=0,-L_y \le y \le 0} = 0 \tag{13}$$

$$\left.\frac{\partial p}{\partial z}\right|_{z=L_z,-L_y \le y \le 0} = 0 \tag{14}$$

3. Resonance Frequency of a Three-Dimensional Cavity Resonance

3.1. Solution to the Vorticity Transfer Equation

We derive the resonance frequency of a two-dimensional cavity resonance. First, we solve equation (1). The solution when the boundary condition is $\zeta(0,t)$ is given by the following equation:

$$\zeta_z(x,y,z,t) = \zeta_z\left(0,0,z,t-\frac{x}{U_{vx}}\right) \tag{15}$$

3.2. Sound Pressure Equation Using Green's Function Derived from Powell's Equation

Next, we solve Powell's equation (2). This can be obtained using the Green's function in the following form. First, the Green's function is given by the following equation.

$$G(x,y,z,t|L_H,0,0,\tau) = \sum_{n=-\infty}^{\infty}\sum_{k=-\infty}^{\infty}\left\{\frac{\delta\left(t-\tau-r_{n,m=0,k}\right)}{4\pi r_{n,m=0,k}} + \frac{\delta\left(t-\tau-r_{n,m=1,k}\right)}{4\pi r_{n,m=1,k}}\right\} \tag{16}$$

Here, the following equation holds true.

$$r_{n,m,k} = \sqrt{(x-(2n+1)L_x)^2 + (y-Y_m)^2 + (z-(2k+1)L_z)^2} \tag{17}$$

$$Y_0 = 0, Y_1 = -2L_y \tag{18}$$

From equations (2) and (16), the following equation is obtained.

$$p(x,y,z,t) = \sum_{n=-\infty}^{\infty} \sum_{k=-\infty}^{\infty} \left[P_{n,m=0,k}(t) + P_{n,m=1,k}(t) \right] \tag{19}$$

Here, the following equation holds true.

$$P_{n,m,k}(t) = \frac{\rho \beta_x}{4\pi r_{n,m,k}} \left[\frac{1}{c} \frac{\partial}{\partial t} \left\{ \Pi(\tau_{n,m,k}) \Phi_{n,m,k}(\tau_{n,m,k}) \right\} + \frac{1}{r_{n,m,k}} \left\{ \Pi(\tau_{n,m,k}) \Phi_{n,m,k}(\tau_{n,m,k}) \right\} \right] \tag{20}$$

$$\tau_{n,m,k} = t - \frac{r_{n,m,k}}{c} \tag{21}$$

$$\Phi_{n,m,k}(\tau) = \frac{U \cdot (x - (2n+1)L_x) - (-1)^{n+k} \cdot v(L_H, 0, 0, \tau) \cdot (y - Y_m)}{c^2 (t-\tau)^2 - r_{n,m,k}^2} \tag{22}$$

$$\Pi(\tau) = \left. \frac{\partial p}{\partial x} \right|_{0,0,z,\tau - \frac{L_x}{U_{vx}}} \tag{23}$$

3.3. x-Direction Resonance Frequency

Consider the resonance frequency in the x-direction. The time it takes for vorticity to propagate downstream is $\frac{L_H}{U_{vx}}$, and the time it takes for the sound to return upstream is $\frac{L_H}{c}$. Here, the phase synchronization condition is assumed to be: "Let T_x be the period of the sound produced (frequency is $f_x = \frac{1}{T_x}$). The total time taken for one cycle, $\frac{L_H}{U_{vx}} + \frac{L_H}{c}$, is equal to an integer multiple (n_x times) of the sound period, taking into account the fluid-induced generation delay (phase difference ϕ)." In this case, the following equation holds:

$$\left(n_x - \frac{\phi}{2\pi} \right) T_x = \frac{L_H}{U_{vx}} + \frac{L_H}{c}$$

$$\frac{\left(n_x - \frac{\phi}{2\pi} \right)}{f_x} = \frac{L_H}{U_{vx}} + \frac{L_H}{c}$$

$$f_x = \frac{\left(n_x - \frac{\phi}{2\pi} \right)}{\frac{L_H}{U_{vx}} + \frac{L_H}{c}} \tag{24}$$

Finally, setting $U_{vx} = \kappa U$, we obtain the following equation. This is Rossiter formula.

$$f_x = \frac{U}{L_H} \frac{\left(n_x - \frac{\phi}{2\pi} \right)}{\left(\frac{1}{\kappa} + \frac{U}{c} \right)} \tag{25}$$

3.4. x-Direction and y-Direction Resonance Frequency

The basic formula for the y-direction resonance frequency f_y of an open-end and closed-end tube in stationary space is as follows:

$$f_y = \frac{(2n_y - 1) \cdot c}{4L_y} \tag{26}$$

3.5. x-Direction and z-Direction Resonance Frequency

The basic formula for the x-direction resonance frequency f_{xr} of a closed tube in stationary space is as follows:

$$f_{xr} = \frac{n_{xr} \cdot c}{2L_x} \tag{27}$$

The resonance frequency in the z direction can be considered in the same way as the resonance frequency in the x direction and is given by the following equation.

$$\therefore f_z = \frac{n_z \cdot c}{2L_z} \tag{28}$$

3.6. Three-Dimensional Resonant Frequencies

The three-dimensional resonance frequency f_{total} is given by the following equation:

$$f_{total} = \sqrt{\left(\frac{n_{xr} \cdot c}{2L_x}\right)^2 + \left(\frac{(2n_y - 1) \cdot c}{4L_y}\right)^2 + \left(\frac{n_z \cdot c}{2L_z}\right)^2} \tag{29}$$

The sound pressure increases at this resonance frequency f_{total}.

3.7. Sound Pressure at a Position Outside the Sound Source ($x \geq L_x$)

We will now discuss the sound pressure at a position outside the sound source ($x \geq L_x$). As before, it can be calculated using the following equation.

$$p(x,y,z,t) = \int_0^{L_z} -\frac{\rho\beta_x}{4\pi r_{3D}(z')}\left\{\frac{1}{c}\frac{\partial}{\partial t}\left[\left.\frac{\partial p}{\partial x}\right|_{\left(0,0,z'\ \tau_{3D}-\frac{L_x}{U_{vx}}\right)} \cdot \Phi_{3D}(x,y,z',\tau_{3D})\right]\right.$$
$$\left. + \frac{1}{r_{3D}(z')}\left[\left.\frac{\partial p}{\partial x}\right|_{\left(0,0,z'\ \tau_{3D}-\frac{L_x}{U_{vx}}\right)} \cdot \Phi_{3D}(x,y,z',\tau_{3D})\right]\right\} dz' \tag{30}$$

Here, the following equation holds.

$$r_{3D}(z') = \sqrt{(x - L_x)^2 + y^2 + (z - z')^2} \tag{31}$$

$$\tau_{3D} = t - \frac{r_{3D}(z')}{c} \tag{32}$$

$$\Phi_{3D}(x,y,z',\tau_{3D}) = U \cdot (x - L_x) - v(L_x, 0, z', \tau_{3D}) \cdot y \tag{33}$$

4. Numerical Calculations

The results were confirmed by numerical calculation. The values used are shown in Table 1 below.

Furthermore, for $\frac{\partial p}{\partial x}$ and $v(L_x, 0, 0, t)$, it was assumed that vortices were continuously generated at the upstream end at a Rossiter formula primary frequency of 14.4 Hz, and that this vortex mass was continuously excited at the downstream end as $v(L_x, 0, z, t)$ at the same Rossiter formula primary frequency of 9.6 (Hz). Therefore, the following equation is continuously used during the numerical calculation. Here, $f_{x,1}$ is the Rossiter formula primary frequency of 9.6 (Hz).

$$\frac{\partial p}{\partial x} = \sin\left(2\pi f_{x,1} t\right) \tag{34}$$

$$v(L_x, 0, z, t) = \frac{1}{2}\sin\left(\frac{\pi z}{L_z}\sqrt{1-\left(\frac{U}{c}\right)^2}\right)\sin\left(2\pi f_{x,1} t\right) \tag{35}$$

Table 1 Parameter and Value

Parameter	Value
ρ	1.225(kg/m^3)
c	340.0(m/s)
U	34.0(m/s)
κ	0.6
β_x	0.01
ϕ	$\frac{\pi}{2}$
L_x	1.5(m)
L_y	0.7(m)
L_z	1.3(m)

The numerical calculation results are shown in Fig. 2. The observation position was $(x, y, z) = (0.01, 0.01, 0.01)$ near the origin. The top graph shows the time-series waveform of sound pressure, and the bottom graph shows the frequency characteristics of sound pressure.

Looking at the time-series waveform of sound pressure in Fig. 2, we see that the "sharp wavefront (a delta function without a tail)" of the three-dimensional spherical wave

undergoes infinite diffuse reflection between the four walls (front, back, left, and right). Because the observation point is near the origin (0.01, 0.01, 0.01), countless "sharp blades of reflected waves" bounced off the walls and hit the observation point at extremely high speeds with a time delay. Each time the time derivative captures this, the sound pressure jumps explosively. As a result, the time waveform becomes a complex waveform with countless discontinuous spikes.

Next, examining the frequency characteristics of the sound pressure shown in Fig. 2, a peak corresponding to the first-order frequency of Rossiter's formula f_x appears at 9.6 (Hz). Since the first-order resonance frequency in the x-direction is 113.3 (Hz)—approximately 12 times the Rossiter first-order frequency—harmonics corresponding to roughly "multiples of 12" are also selected and resonate, creating small peaks around the solid blue line. Resonance also occurs at $f_y = 364.3$ (Hz) (where $n_y = 2$) and $f_z = 261.5$ (Hz) (where $n_z = 2$).

The reason why the entire red spectrum in the frequency response graph of sound pressure in Fig. 2 does not consist of a single peak of a sine wave, but rather a complex shape with fine irregularities spread across the surface (a spectrum similar to turbulent noise), is because, as predicted by the f_{total} formula above, each infinitely reflected sound responds to every pair of n_x, n_y, n_z (innumerable three-dimensional resonance points), causing the entire space to vibrate finely at all frequencies.

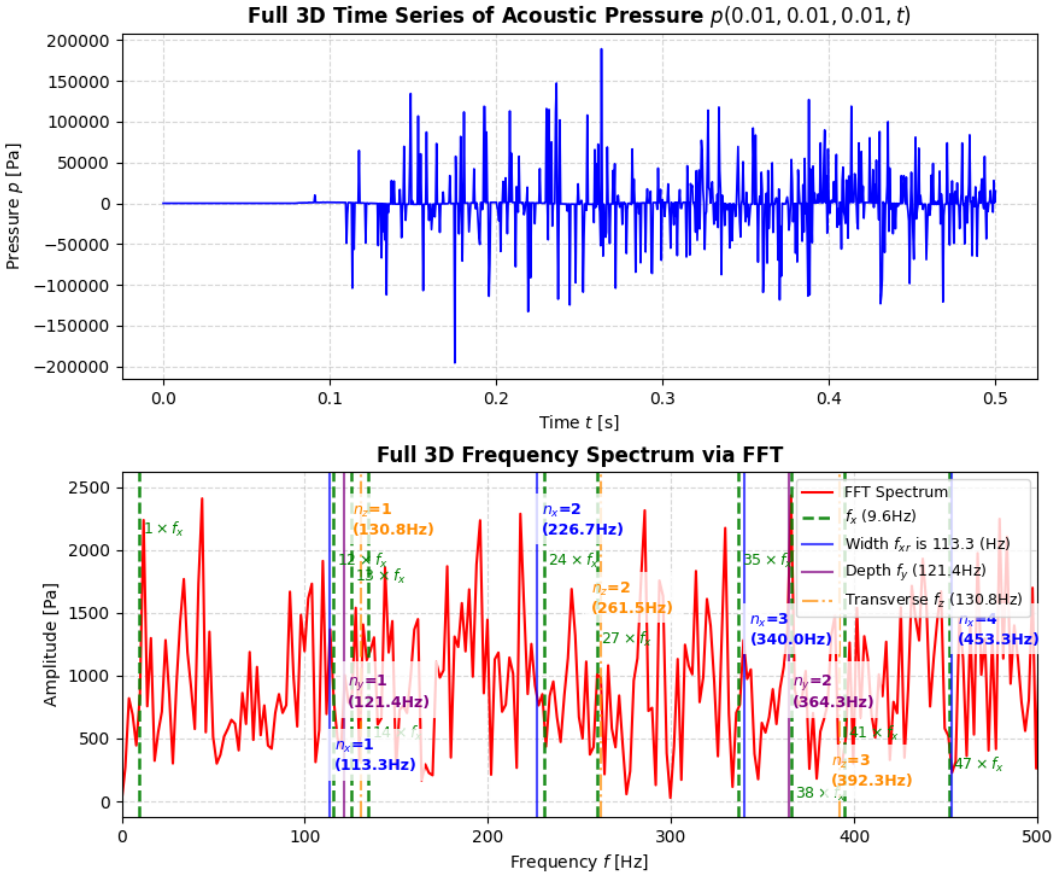

Fig. 2 Numerical Calculation Results

Next, we calculate the sound pressure for $x \geq L_x$. The results are shown in Fig. 3. The observation position was $(x, y, z) = (2.0, 0.5, 0.6)$. The top graph shows the time-series waveform of the sound pressure, and the bottom graph shows the frequency response of the sound pressure.

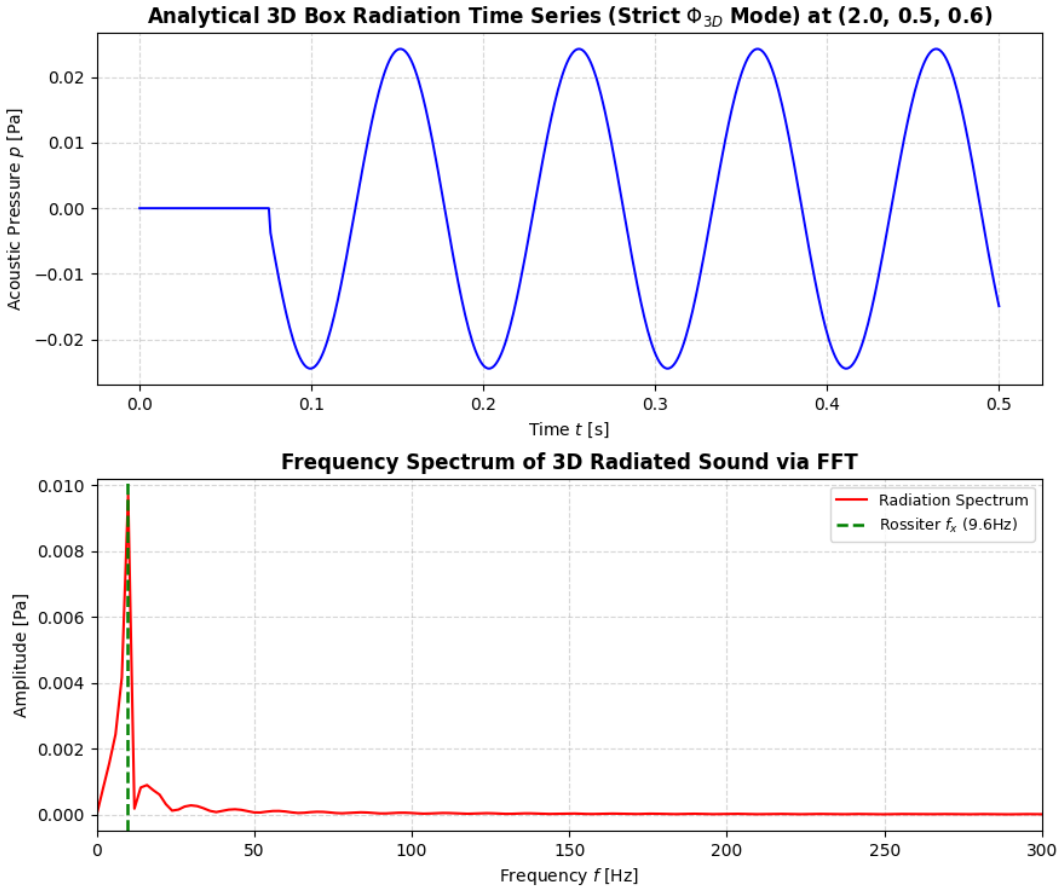

Fig. 3 Numerical Calculation Result ($(x, y, z) = (2.0, 0.5, 0.6)$)

Looking at the top graph in Fig. 3, we can see that time is required for the sound to reach the source. Also, from the frequency response below, a peak at 9.6 (Hz) appears, corresponding to the first frequency of Rossiter formula f_x. That is, for $x \geq L_x$, the sound has a frequency component at the first frequency of Rossiter formula f_x, which is the frequency of forced oscillation.

Finally, Fig. 4 shows the numerical calculation results when the observation position is (x, y, z) = (0.01, 0.01, 0.01) near the origin when $U = 340.0$ (m/s). There is a large peak at the primary resonance frequency of f_x. There are also peaks in f_{xr}, f_y, and f_z. I tried to reproduce the lock-in phenomenon by making U faster than this, but the calculations diverged and I could not obtain numerical results.

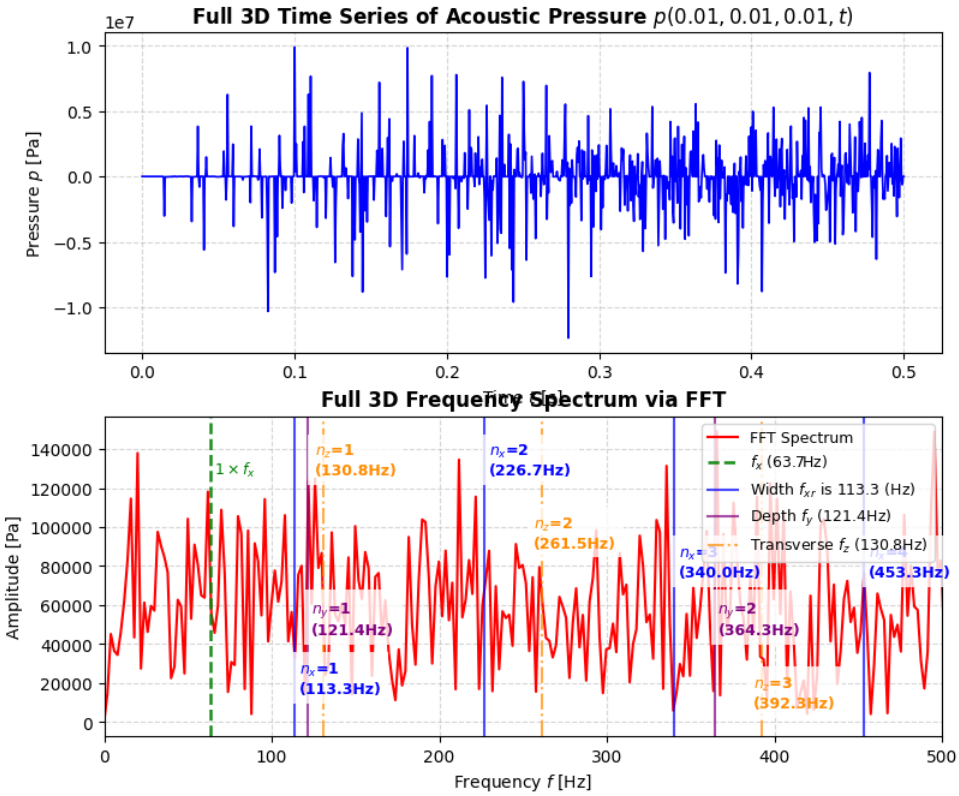

Fig. 4 Numerical Calculation Result (U = 340.0(m/s))

5. Conclusion

Research on automobile whistling and suction sounds has been conducted in the past. For cavity resonance, a type of whistling sound, the cavity resonance frequency has been determined using Rossiter's empirical equation. Therefore, we limited our study to the three-dimensional case and clarified the physical phenomena that arise by solving a set of partial differential equations that explain the phenomenon. As a result, we were able to determine the frequency at which resonance increases, taking into account three-dimensional space. Finally, we were able to confirm the conditions under which resonance increases through numerical calculations.

References

Calvo, J. A., Diaz, V., & San Roman, J. L. (2005). *Controlling the turbocharger whistling noise in diesel engines.* International Journal of Vehicle Noise and Vibration, Vol. 2, No. 1. doi:https://doi.org/10.1504/IJVNV.2006.008524

Chien-Hsiung, T., Lung-Ming , F., Chang-Hsien , T., Yen-Loung , H., & Jik-Chang , L. (2009). *Computational aero-acoustic analysis of a passenger car with a rear spoiler.* Applied Mathematical Modelling, Volume 33, Issue 9. doi:https://doi.org/10.1016/j.apm.2008.12.004

George, A. R. (1990). *Automobile Aerodynamic Noise.* SAE Transactions, Vol. 99, Section 6. Retrieved from http://www.jstor.org/stable/44553993

Jagtiani, H. (1972). *The Objective Method of Evaluating Aspiration Wind Noise.* SAE Technical Paper 720506. doi:https://doi.org/10.4271/720506

Jung, W., & Oh, S. (1995). *The Influence of Vehicle Elements to Aspiration Wind Noise.* SAE Technical Paper 950624. doi:https://doi.org/10.4271/950624

Münder, M., & Carbon, C.-C. (2022). *Howl, whirr, and whistle: The perception of electric powertrain noise and its importance for perceived quality in electrified vehicles.* Applied Acoustics, Volume 185. doi:https://doi.org/10.1016/j.apacoust.2021.108412

Oettle, N., & Sims-Williams, D. (2017). *Automotive aeroacoustics: An overview.* Journal of Automobile Engineering, Volume 231, Issue 9. doi:https://doi.org/10.1177/0954407017695147

Qatu, M. S., Abdelhamid, M. K., Pang, J., & Sheng, G. (2009). *Overview of automotive noise and vibration.* International Journal of Vehicle Noise and Vibration, Vol. 5, No. 1-2. doi:https://doi.org/10.1504/IJVNV.2009.029187

Wang, Q., Chen, X., & Zhang, Y. (2021). *An Overview of Automotive Wind Noise and Buffeting Active Control.* SAE International Journal of Vehicle Dynamics, Stability, and NVH, 5(4). doi:https://doi.org/10.4271/10-05-04-0030

Zhang, F., Meng, W., Li, X., & Zheng, C. (2022). *A vehicle whistle database for evaluation of outdoor acoustic source localization and tracking using an intermediate-sized microphone array.* Applied Acoustics, Volume 201. doi:https://doi.org/10.1016/j.apacoust.2022.109113